Abstract number: 688278
2021 INTERNATIONAL OIL SPILL CONFERENCE

Experimental and computational study of oil jet in crossflow

Cosan Daskiran[1], Fangda Cui[1], Lin Zhao[2§], Scott A. Socolofsky[3], Kenneth Lee[4], Michel C. Boufadel[1*]

[1]*Center for Natural Resources, Civil and Environmental Engineering Department, New Jersey Institute of Technology, Newark, NJ 07102*

[2] *ExxonMobil Upstream Research Company, Houston, TX 77389*

[3]*Zachry Department of Civil Engineering, Texas A&M University, College Station, TX 77843*

[4]*Bedford Institute of Oceanography, Department of Fisheries and Oceans, Dartmouth, Canada*

[*]Corresponding author: *Michel C. Boufadel (boufadel@gmail.com; http://nrdp.njit.edu)*

[§]Work was completed while the author was a Postdoctoral Researcher at the New Jersey Institute of Technology

Abstract

During undersea oil blowout in crossflow conditions, the oil droplets entrained horizontally which increased the residence time of droplets in the water column. Knowledge of the trajectory of an oil plume is important for predicting the pathways of hydrocarbons and to devise countermeasures. We conducted large-scale experiments in the Ohmsett tank where we released oil from a one-inch vertical orifice that was towed to produce the behavior of a jet in crossflow. The average oil velocity at the orifice was 1.36 m/s and the crossflow velocity was around 0.27 m/s which resulted in a jet-to-crossflow velocity ratio of 5.0. The results were simulated numerically using the Large Eddy Simulation (LES) turbulence model and the mixture multiphase model within the open-source software OpenFOAM. The instruments including ADVs, LISSTs, shadowgraph cameras, holographic camera, and fluorometers were employed. The oil jet released from the nozzle started to meander in the vertical direction most probably due to weak crossflow. The trajectory and meandering behavior of the oil jet, wavy pattern along the leading edge of the jet and column breakup observed in the experiments were captured well with the numerical simulation. The surface breakup just above the orifice created ligaments and droplets downstream of the jet. Larger oil droplets were observed near the upper boundary of the plume due to their higher buoyancy while the smaller droplets were suspended in the water column and they were entrained by water crossflow. This work reveals that different size of droplets determines the overall shape of plumes mostly the upper and lower boundaries of the plume.

1 Introduction

The Deepwater Horizon oil spill in 2010 is recognized to be the worst environmental disaster in U.S. history with an estimated oil release of 4.9 to 6.2 million barrels (Griffiths 2012), and highlighted the need for a better understanding of underwater oil jets and plumes. A comprehensive review for droplets, hydrodynamics and chemistry of multiphase jets/plumes including recent numerical and experimental studies was conducted by Boufadel et al. (2020). Due to horizontal currents in the ocean, the released jet could bend horizontally causing the oil droplets and gas bubbles to separate from it. In spite of the importance of this behavior on the trajectory and fate of oil, there is little understanding of the residence time of the droplets within the plume, which is likely to be increased due to turbulence. For this reason, we report herein the results of an experimental release of oil at 40 liter/min from a one-inch pipe in the Ohmsett tank in New Jersey. The experimental results were simulated using high-fidelity (20 million cells) large eddy simulation turbulence model and mixture multiphase model.

The droplet size is crucial to estimate the trajectory and the residence time of the droplets in the water column which becomes important for the oil spill response team to set the countermeasures. Based on the estimated trajectory of oil droplets, the region to apply underwater dispersant can be determined more precisely. The dispersant is used to decrease the interfacial tension between oil and water and creates smaller droplets. The decrease in the droplet size decreases the rise velocity of droplets and increases their residence time in the water column which increases the biodegradation and dissolution rate of oil droplets into water. In addition to the underwater dispersant application, estimating the location of the oil slick before the droplets reach the water surface provides additional time for the response team to get prepared for the countermeasures. The density stratification and horizontal streams in the water column have a major role on oil transport. The role of waves on the transport of surfaced oil droplets was investigated in our recent work (Cui et al. 2020a, Cui et al. 2020b). In this work, we focused on the influence of horizontal crossflows on oil trajectory. Another crucial parameter for numerical models to estimate oil trajectory accurately is the initial droplet size which was considered to be generated through the shear among water and oil and resulting Kevin-Helmholtz instabilities above the orifice (within a few diameters) (Funada et al. 2004, Bo et al. 2011, Xue and Katz 2019).

Daskiran et al. (2020a) investigated the formation of ligaments and droplets in the shear breakup (also called primary breakup) zone.

Jets penetrate into the crossflow based on their initial momentum and starts bending in the crossflow direction. The flow field and vortical structures have been characterized through numerical and experimental studies from small-scale jets (Yuan et al. 1999, Gopalan et al. 2004, Muppidi and Mahesh 2007, Mahesh 2013, Behzad et al. 2016). Yuan et al. (1999) observed rollers in a spanwise direction near the leading and trailing edges of the jet due to the Kelvin Helmholtz (K-H) instabilities which occur at the phase interface due to the velocity difference. Muppidi and Mahesh (2007) investigated turbulent kinetic energy budgets through direct numerical simulations. In the near field of the jet, they observed peak kinetic energy production near the leading edge of the jet and peak energy dissipation rate near the trailing edge of the jet. Gopalan et al. (2004) characterized the jet in crossflow based on the velocity ratio, *r*, the ratio of jet velocity to crossflow velocity. They reported a semi-cylindrical vortical layer with a reverse flow behind the jet for the velocity ratio smaller than 2.0. They did not observe the reverse flow for higher velocity ratios. Instead, they observed vortical structures behind the jet similar to Karman vortex street. Behzad et al. (2016) investigated the surface breakup and the formation of ligaments and droplets from the jet shear layer due to the azimuthal instabilities along the jet periphery. Many studies for the jet in crossflow were performed as single-phase or multiphase such as liquid jet in gaseous crossflow. Murphy et al. (2016) investigated oil jet in crossflow experimentally by towing the pipe and investigating the water velocity (and oil velocity) using Particle Image velocimetry (PIV). They revealed and quantified the vertical velocity induced by a counter-rotating vortex pair (CVP) beneath the plume. Recently, Daskiran et al. (2020b, 2021) conducted a large eddy simulation and reported detailed hydrodynamics of jet in crossflow and the role of CVP on oil distribution and mixing. Using the hydrodynamics from the LES, Daskiran et al. (2020c) carried out Lagrangian particle tracking simulations using their in-house code "NEMO3D" (Cui et al. 2018, Cui et al. 2020a). They investigated the transport of droplets in various sizes and trapping of small droplets (i.e. a few hundred microns) inside the CVP.

The objective of this work is to compare large-scale experiments of the oil jet in crossflow to

numerical simulations. To the best knowledge of the authors, there are not sufficient number of studies for large-scale multiphase liquid-liquid jet flows in crossflows. This work will aid in estimating the oil trajectory and overall shape of plumes mostly the upper and lower boundaries of the plume in crossflow.

2 Experimental and simulation Setup

The experiments of the jet in crossflow were conducted at Ohmsett wave tank facility which has 203 m length, 20 m width and 2.4 m depth. The oil type used in the experiments was Fuel oil #2. The properties of the oil and seawater were provided in Table 1. The parameter *D* in Table 1 represents the pipe diameter. In addition to the experiments, large eddy simulation was performed for the same flow conditions.

Table 1. The properties of oil and seawater used in the experiment and simulation.

ρ_{oil}	ρ_{water} [kg/m^3]	μ_{oil} [cP]	μ_{water} [cP]	σ [mN/m]	D [mm]
840	*1025*	*4*	*1.1*	*25.6*	*25*

In the experiments, the pipe and the instruments were towed to mimic the crossflow current. Several instruments were installed on the metallic frames downstream of the orifice to measure flow velocity, oil droplet size and oil concentration in water. Figure 1 shows the snapshots of the metallic frame with different instruments installed. Four Acoustic Doppler Velocimetry (ADV) were installed to measure velocity in three-dimensions as a function of time at specified measurement points. Three LISSTs (Laser in-situ scattering and transmissometry), two LISST-100X and one LISST-200X, were installed to reveal the oil droplet size distribution (DSD) in the range of 2.5-500 micron. Two shadowgraph cameras were employed to capture the droplets larger than 500 microns. The shadowgraph cameras used herein are telecentric and consist of two cylindrical parts with a gap between to allow the oil droplets pass through. One side of the camera is the light source while the other side includes the camera. The images of droplets were taken while they are passing through the gap with a frequency of 10 Hz. The holographic camera was also installed to capture images of droplets. Two fluorometers named “Wetlab SeaOWL” and “Turner Cyclops C7” were used to measure dissolved oil concentration in water. The LISSTs and the cameras were installed carefully to measure the droplet size across the plume cross-section particularly near the upper and lower boundaries of the plume.

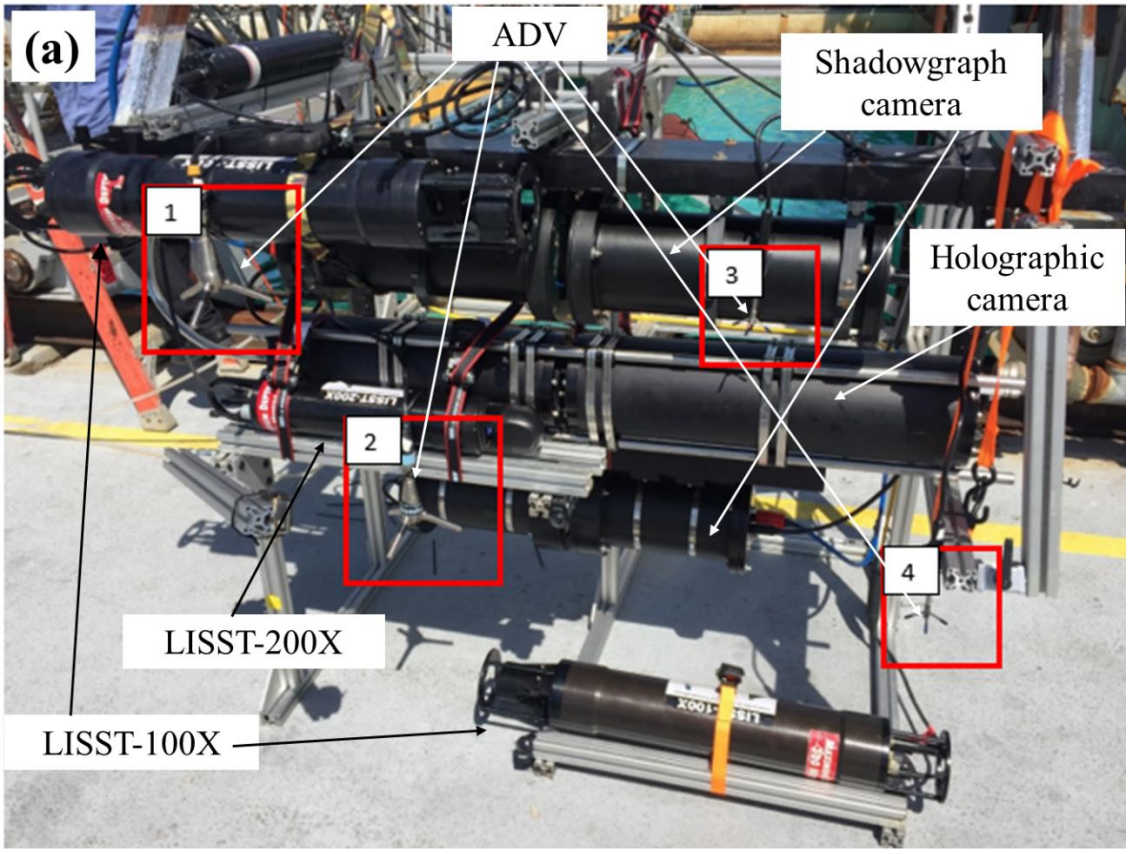

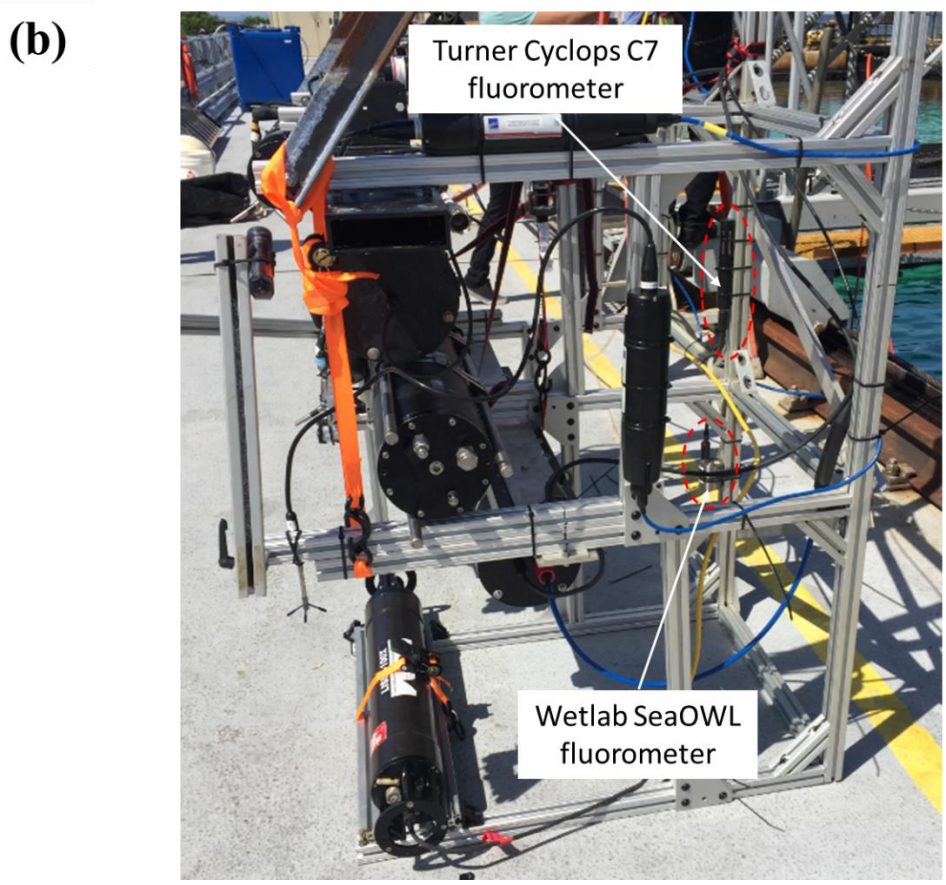

Figure 1. Location and setup of the instruments mounted on metallic frames. Four ADVs, three LISSTs, two shadowgraph cameras, one holographic camera and two fluorometers were used.

In the simulation, a rectangular computational domain was employed. The oil was injected in the vertical direction while crossflow was moving in the horizontal direction. The pipe length was 20*D* and the vertical distance between the orifice and water free surface was roughly 70*D*. The pipe was placed 160*D* away from the water channel inlet. The distance between the pipe and channel outlet was 240*D* to allow the oil jet to bend in the crossflow direction. At the water inlet, a crossflow velocity of 0.27 m/s was used. At the pipe inlet, oil had an average velocity of 1.36 m/s which corresponds to an oil flow rate of 40 liters/min. At the outlet, a zero-gradient condition was applied for the velocity in the direction normal to the surface. Zero-shear wall and no-slip wall boundary conditions were employed for the side boundaries of the computational domain and the pipe wall, respectively. The number of cells used in the simulation was around 20 million. The cell size was refined carefully near the orifice and in the region occupied by the plume.

In the simulation, open-source computational fluid dynamics software, OpenFoam, was utilized. The mixture multiphase model (Manninen et al. 1996) and high-fidelity large eddy simulation (LES) turbulence model were employed to track the oil droplets in the turbulent flow field. In LES model, second order discretization schemes were used for all the equations except for the time discretization. First-order discretization scheme was used for the time ensuring a maximum Courant number of 1.0. The time step size was around 7.2×10^{-5} s as the flow reached quasi-steady behavior.

3 Results and Discussion

Underwater oil blowouts including jets or plumes emanating into the stationary ambient environment were studied by our group (Zhao et al. 2014a, Zhao et al. 2014b, Zhao et al. 2016, Gao et al. 2017, Zhao et al. 2017a, Zhao et al. 2017b, Boufadel et al. 2018). The engineering models named VDROP and VDROP-J estimating droplet size distribution were proposed and validated against experimental measurements. The flow characteristics for a vertical jet into crossflow differs from the jet into a stationary flow based on different types of vortices including horseshoe vortices, wake vortices and counter-rotating vortex pair (Fric and Roshko 1994).

Figure 2 illustrates the time series of snapshots acquired during the experiments. Initially (at t=0 s), a vertical jet was obtained and waited for more than 10 s to allow the plume to reach quasi-steady

behavior before starting to tow. The towing direction was from right to left to mimic the crossflow from left to right. The dynamic response of the jet to the towing can be seen in Figure 2b-d. The upstream portion of the plume started to bend last. After almost 11 s, the plume takes its tilted shape within the crossflow direction. The horizontal and vertical distances between the pipe orifice and the instruments were decided attentively to allow the plume to pass through the instruments.

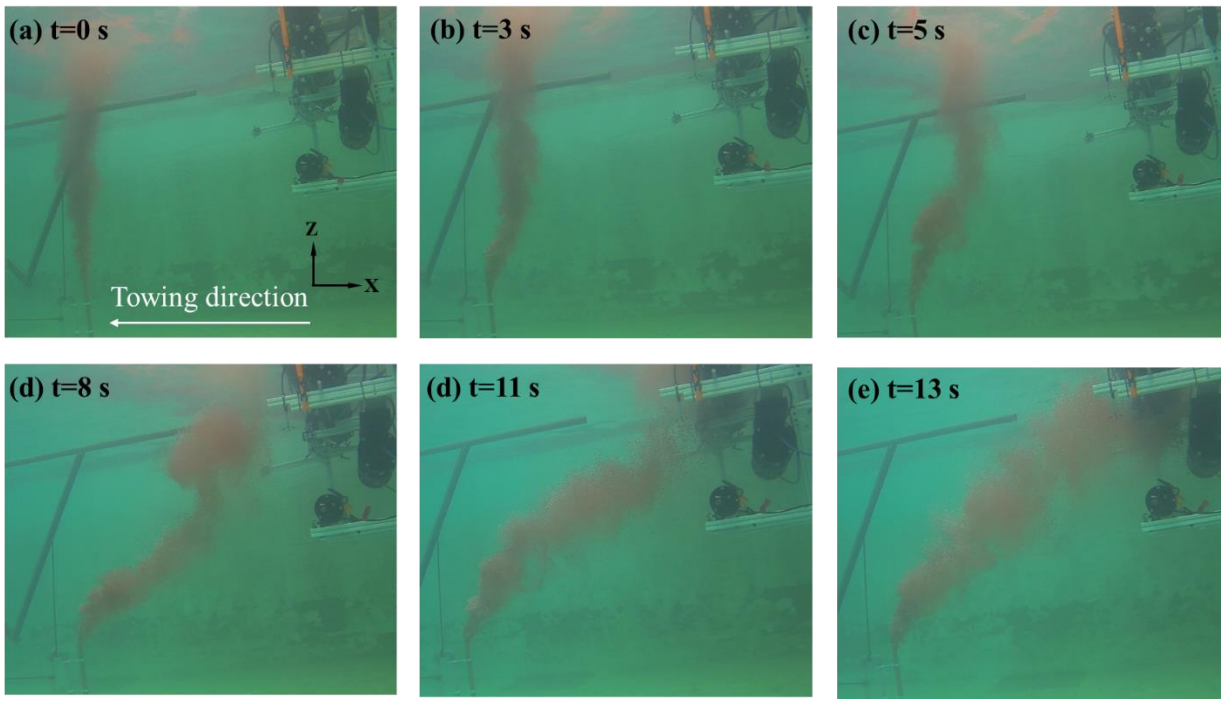

Figure 2. Snapshots from the experiment of oil jet in crossflow in consequent times. The jet was started in the vertical direction initially. The time t=0 represents the time when the towing was started.

The snapshot in Figure 3 reveals the trajectory of the oil plume in the crossflow. Both the upper and lower boundaries of the plume meander in the vertical direction which is clearer in the movies. The oil jet was almost vertical within 2-3*D* from the orifice, then started bending in the direction of the crossflow as its momentum decayed. The wave peaks along the leading edge of the jet, which were induced by K-H instabilities, were clear and continuous up to 10*D* from the orifice in the vertical direction. The length of the waves increased in the direction of the jet path. The axial disturbances induced by the interaction between the jet and crossflow, and the meandering behavior of the jet lead to the column breakup which can be characterized by the disintegration of the jet core into large chunks of oil (Behzad et al. 2016). As the far-field of the plume was focalized, the discrete large droplets were observed near the upper boundary of the plume. In immiscible flows, the discrete droplets can separate

158 from the continuous flow due to buoyancy, turbulence and stratification (Socolofsky et al. 2002).
159 Therefore, larger droplets in the plume identify the upper boundary of the plume.

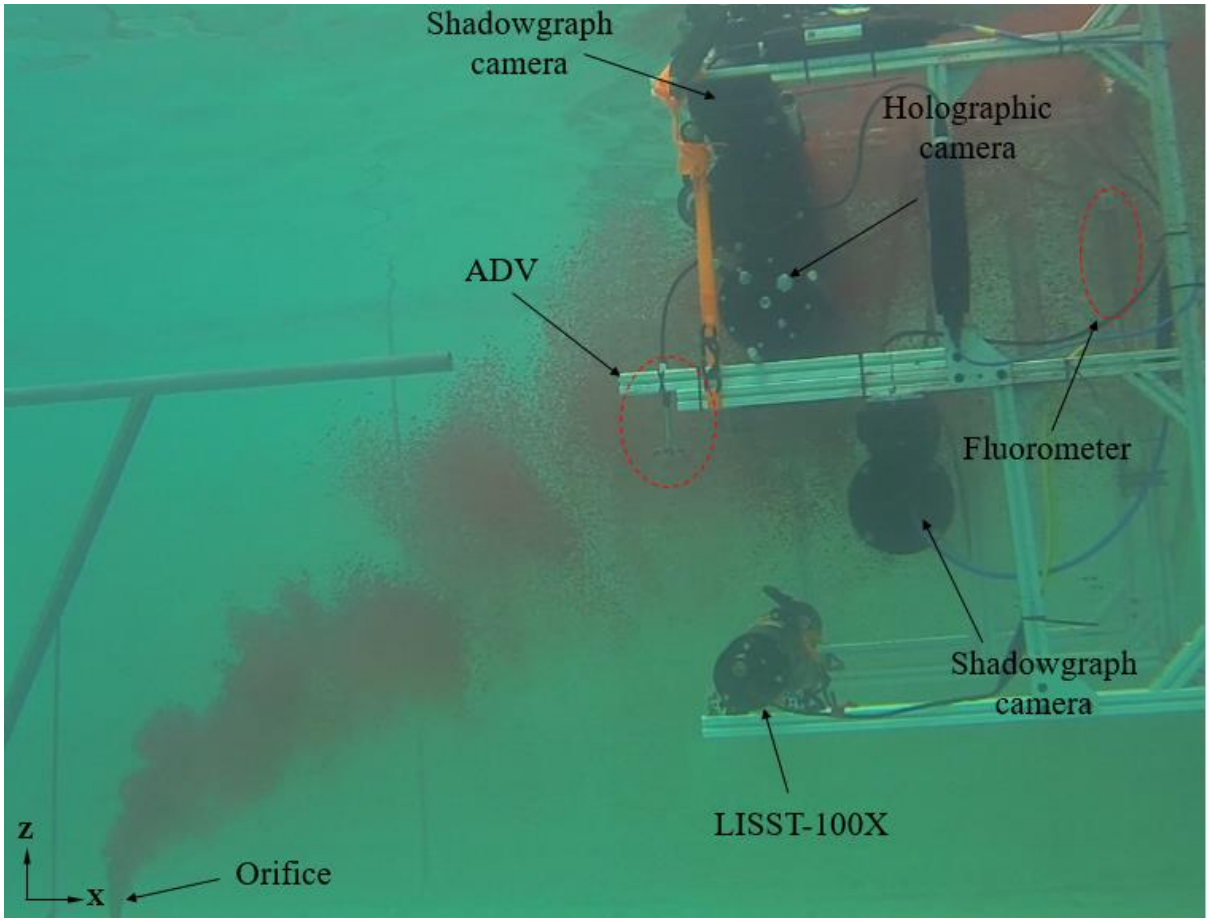

160

161 Figure 3. Snapshot from the experiment of oil jet in crossflow. The oil flow rate is 40 liters/min.

162 Four ADVs (Nortek AS) were utilized to measure the instantaneous velocity components at
163 different locations. The accuracy of the ADV data can be evaluated based on signal to noise ratio (SNR)
164 and correlation coefficient. The SNR is related to the particle seeding concentration while the
165 correlation reveals the uncertainty in the velocity data. A higher correlation coefficient provides velocity
166 at higher accuracy (Mori et al. 2007). The SNR>5 is required to acquire the mean velocity while the
167 SNR>15 is a necessity for instant velocity data (Nortek 1998, McLelland and Nicholas 2000).
168 McLelland and Nicholas (2000) suggested a correlation coefficient of 60% or higher for accurate
169 velocity output. Figure 4 illustrates the time series of velocity components acquired from the ADV-3
170 labeled in Figure 1. The velocity data having SNR<15 and correlation coefficient smaller than 60%
171 were excluded. The ADV-3 measures the velocity at (x,y,z)=(1.55 m, 0.34 m, 1.29 m) based on the

origin (0,0,0) located at the center of the pipe orifice. The crossflow is in the *x*-direction while the oil jet is in the *z*-direction, see Figure 3. The towing speed was 0.27 m/s and the horizontal velocity in Figure 4a oscillates around ~0.3 m/s. The unsteady deviation from the mean velocity can be related to the meandering behavior of the plume, see Figure 3. The amplitude of the vertical velocity fluctuations was measured to be smaller than that of horizontal velocity. The vertical velocity was measured to be around 0.1 m/s. The vertical velocity for the jet in crossflow has three components: (1) jet momentum in vertical direction, (2) rise (slip) velocity of droplets and (3) flow induced by counter rotating vortex pair (Murphy et al. 2016). The velocity in lateral direction oscillates around 0 m/s between -0.1 m/s and 0.1 m/s.

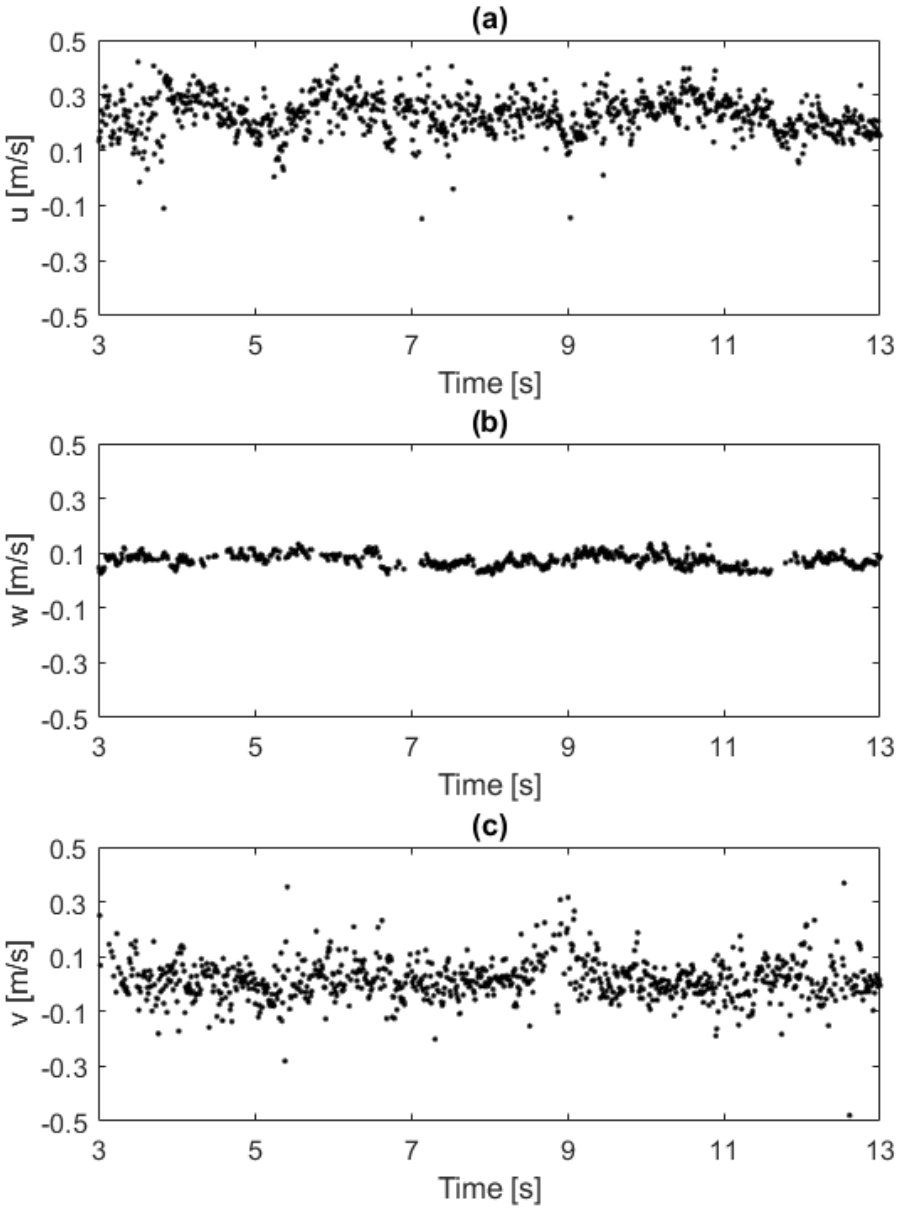

Figure 4. Time series of velocity in different directions measured by the ADV numbered 3 in Figure 1. The velocities u, v and w represent the velocities in horizontal, lateral and vertical directions. The ADV-3 measures velocity at (x,y,z)=(1.55 m, 0.34 m, 1.29 m) based on the origin (0,0,0) located at the center of pipe orifice. The figure was obtained from Daskiran et al. (2020b).

Figure 5 illustrates the numerical predictions of instantaneous oil holdup along the symmetry plane. The near-field of the jet was magnified and placed top-left. The trajectory and meandering behavior of the jet, wavy pattern along the leading edge of the jet and the column breakup of the plume observed in the experiments captured well within the simulations. Initially, the jet moved in the vertical direction and bent in the horizontal direction slightly up to 3*D* from the orifice. The jet completed its bending smoothly within 10*D* from the orifice and raised almost with a constant slope. The wavy behavior induced by K-H instabilities was observed near the leading edge of the jet and lasted nearly 10*D*. Following the wavy pattern, column break was observed due to axial disturbances (Behzad et al. 2016). In the near field of the jet, the surface breakup induced by azimuthal instabilities created ligaments and droplets along the trailing edge of the jet (Behzad et al. 2016). The dilution of oil along the jet path was also quantified. At 30*D* away from the pipe orifice, the oil holdup decreased to 0.1. As the plume diluted more, the distance between the oil pockets was increased. The oil holdup was estimated to be higher near the upper boundary of the plume.

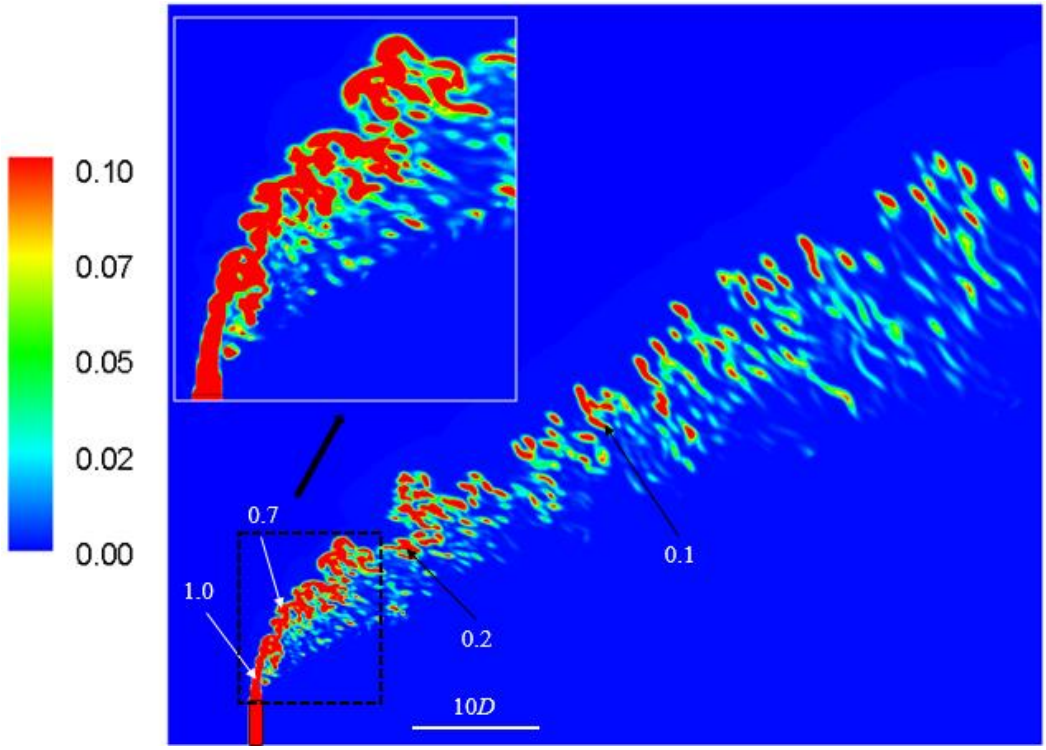

Figure 5. Instantaneous contours of oil holdup at t=10 s. The oil is discharged into the streaming water from a pipe with a diameter of 2.5 cm. The water stream is in $+x$ direction while the oil jet is in $+z$ direction.

4 Conclusions

Large scale experiments of oil jet in crossflow were performed at Ohmsett wave tank facility and simulated herein through the computational fluid dynamics approach. Several instruments including ADVs, LISSTs, shadowgraph cameras, holographic camera, and fluorometers were used in the experiments. In contrast to most of the prior studies, a larger orifice with a diameter of one-inch was used in this work which is crucial to adjust correlations that were proposed to estimate median droplet size (d_{50}). Li et al. (2017) argued that using the same correlations for a relatively larger pipe diameter might result in a droplet diameter larger than the maximum stable droplet size. Using both LISST and shadowgraph cameras in this work aids in capturing the whole droplet size range from 1.0 μm to cm scale.

The trajectory and meandering behavior of the oil jet, wavy pattern along the leading edge of the jet and column breakup observed in the experiments were captured well with the numerical simulation. The surface breakup near-field of the jet induced by azimuthal instabilities created ligaments and droplets downstream of the trailing edge of the jet. Larger oil droplets escaped from the entrained water and they were observed near the upper boundary of the plume since the larger droplets have higher buoyancy (Boufadel et al. 2007) to overcome the turbulent mixing while the smaller droplets were suspended and tracked the water flow.

Acknowledgment

The authors gratefully acknowledge support by the Department of Fisheries and Oceans (DFO) Canada through the Multi-Partner Research Initiative grant: MECTS-39390783-v1-OFSCP. Funding from the Centre for Offshore Oil, Gas and Energy Research (COOGER) and the Gulf of Mexico Research Initiative (GOMRI) are also acknowledged. This work used the Extreme Science and Engineering Discovery Environment (XSEDE), which is supported by the National Science Foundation grant number TG-BCS190002. Specifically, we used the *Comet* system, which is operated by the San Diego

Supercomputer Center at UC San Diego and the *Bridges* system at the Pittsburgh Supercomputing Center (PSC).

5 References

Behzad, M., N. Ashgriz and B. Karney (2016). "Surface breakup of a non-turbulent liquid jet injected into a high pressure gaseous crossflow." International Journal of Multiphase Flow **80**: 100-117.

Bo, W., X. Liu, J. Glimm and X. Li (2011). "A robust front tracking method: verification and application to simulation of the primary breakup of a liquid jet." SIAM Journal on Scientific Computing **33**(4): 1505-1524.

Boufadel, M. C., K. Du, V. Kaku and J. Weaver (2007). "Lagrangian simulation of oil droplets transport due to regular waves." Environmental Modelling & Software **22**(7): 978-986.

Boufadel, M. C., F. Gao, L. Zhao, T. Özgökmen, R. Miller, T. King, B. Robinson, K. Lee and I. Leifer (2018). "Was the Deepwater Horizon well discharge churn flow? Implications on the estimation of the oil discharge and droplet size distribution." Geophysical Research Letters **45**(5): 2396-2403.

Boufadel, M. C., S. Socolofsky, J. Katz, D. Yang, C. Daskiran and W. Dewar (2020). "A Review on Multiphase Underwater Jets and Plumes: Droplets, Hydrodynamics, and Chemistry." Reviews of Geophysics **58**(3): e2020RG000703.

Cui, F., M. C. Boufadel, X. Geng, F. Gao, L. Zhao, T. King and K. Lee (2018). "Oil Droplets Transport Under a Deep-Water Plunging Breaker: Impact of Droplet Inertia." Journal of Geophysical Research: Oceans **123**(12): 9082-9100.

Cui, F., C. Daskiran, T. King, B. Robinson, K. Lee, J. Katz and M. C. Boufadel (2020b). "Modeling oil dispersion under breaking waves. Part I: Wave hydrodynamics." Environmental Fluid Mechanics: 1-25.

Cui, F., L. Zhao, C. Daskiran, T. King, K. Lee, J. Katz and M. C. Boufadel (2020a). "Modeling oil dispersion under breaking waves. Part II: Coupling Lagrangian particle tracking with population balance model." Environmental Fluid Mechanics: 1-26.

Daskiran, C., F. Cui, M. C. Boufadel, R. Liu, L. Zhao, T. Ozgokmen, S. A. Socolofsky and K. Lee (2021). "Computational and experimental study of an oil jet in crossflow: Coupling population balance model with multiphase large eddy simulation." Journal of Fluid Mechanics (Under review).

Daskiran, C., F. Cui, M. C. Boufadel, S. A. Socolofsky, J. Katz, L. Zhao, T. Ozgokmen, B. Robinson and T. King (2020c). "Transport of oil droplets from a jet in crossflow: Dispersion coefficients and Vortex trapping." Ocean Modelling **158**: 101736.

Daskiran, C., F. Cui, M. C. Boufadel, L. Zhao, S. A. Socolofsky, T. Ozgokmen, B. Robinson and T. King (2020b). "Hydrodynamics and dilution of an oil jet in crossflow: The role of small-scale motions from laboratory experiment and large eddy simulations." International Journal of Heat and Fluid Flow **85**: 108634.

Daskiran, C., X. Xue, F. Cui, J. Katz and M. C. Boufadel (2020a). "Large Eddy Simulation and Experiment of Shear Breakup in Liquid-Liquid Jet: Formation of Ligaments and Droplets." International Journal of Heat and Fluid Flow (Under review).

Fric, T. and A. Roshko (1994). "Vortical structure in the wake of a transverse jet." Journal of Fluid Mechanics **279**: 1-47.

Funada, T., D. Joseph and S. Yamashita (2004). "Stability of a liquid jet into incompressible gases and liquids." International journal of multiphase flow **30**(11): 1279-1310.

Gao, F., L. Zhao, M. Boufadel, T. King, B. Robinson, R. Conmy and R. Miller (2017). "Hydrodynamics of oil jets without and with dispersant: Experimental and numerical characterization." Applied Ocean Research **68**: 77-90.

Gopalan, S., B. M. Abraham and J. Katz (2004). "The structure of a jet in cross flow at low velocity ratios." Physics of fluids **16**(6): 2067-2087.

Griffiths, S. K. (2012). "Oil release from Macondo well MC252 following the Deepwater Horizon accident." Environmental science & technology **46**(10): 5616-5622.

Li, Z., M. Spaulding, D. French McCay, D. Crowley and J. R. Payne (2017). "Development of a unified oil droplet size distribution model with application to surface breaking waves and subsea blowout releases considering dispersant effects." Marine Pollution Bulletin **114**(1): 247-257.

Mahesh, K. (2013). "The interaction of jets with crossflow." Annual review of fluid mechanics **45**: 379-407.

Manninen, M., V. Taivassalo and S. Kallio (1996). On the mixture model for multiphase flow, Technical Research Centre of Finland Finland.

McLelland, S. J. and A. P. Nicholas (2000). "A new method for evaluating errors in high-frequency ADV measurements." Hydrological processes **14**(2): 351-366.

Mori, N., T. Suzuki and S. Kakuno (2007). "Noise of acoustic Doppler velocimeter data in bubbly flows." Journal of engineering mechanics **133**(1): 122-125.

Muppidi, S. and K. Mahesh (2007). "Direct numerical simulation of round turbulent jets in crossflow." Journal of Fluid Mechanics **574**: 59-84.

Murphy, D. W., X. Xue, K. Sampath and J. Katz (2016). "Crude oil jets in crossflow: Effects of dispersant concentration on plume behavior." Journal of Geophysical Research: Oceans **121**(6): 4264-4281.

Nortek, A. (1998). "ADV operation manual." Vollen, Norway **34**.

Socolofsky, S. A., B. C. Crounse and E. E. Adams (2002). Multiphase plumes in uniform, stratified, and flowing environments, ASCE Reston, Va.

Xue, X. and J. Katz (2019). "Formation of compound droplets during fragmentation of turbulent buoyant oil jet in water." Journal of Fluid mechanics **878**: 98-112.

Yuan, L. L., R. L. Street and J. H. Ferziger (1999). "Large-eddy simulations of a round jet in crossflow." Journal of Fluid Mechanics **379**: 71-104.

Zhao, L., M. C. Boufadel, T. King, B. Robinson, F. Gao, S. A. Socolofsky and K. Lee (2017a). "Droplet and bubble formation of combined oil and gas releases in subsea blowouts." Marine Pollution Bulletin **120**(1-2): 203-216.

Zhao, L., M. C. Boufadel, S. A. Socolofsky, E. Adams, T. King and K. Lee (2014b). "Evolution of droplets in subsea oil and gas blowouts: Development and validation of the numerical model VDROP-J." Marine Pollution Bulletin **83**(1): 58-69.

Zhao, L., F. Gao, M. C. Boufadel, T. King, B. Robinson, K. Lee and R. Conmy (2017b). "Oil jet with dispersant: Macro-scale hydrodynamics and tip streaming." AIChE Journal **63**(11): 5222-5234.

Zhao, L., F. Shaffer, B. Robinson, T. King, C. D'Ambrose, Z. Pan, F. Gao, R. S. Miller, R. N. Conmy and M. C. Boufadel (2016). "Underwater oil jet: Hydrodynamics and droplet size distribution." Chemical Engineering Journal **299**: 292-303.

Zhao, L., J. Torlapati, M. C. Boufadel, T. King, B. Robinson and K. Lee (2014a). "VDROP: A comprehensive model for droplet formation of oils and gases in liquids-Incorporation of the interfacial tension and droplet viscosity." Chemical Engineering Journal **253**: 93-106.